NMR solution structure of BmK-βIT, an excitatory scorpion β-toxin without a 'hot spot' at the relevant position

ARTICLE *in* BIOCHEMICAL AND BIOPHYSICAL RESEARCH COMMUNICATIONS · NOVEMBER 2006

Impact Factor: 2.3 · DOI: 10.1016/j.bbrc.2006.08.131 · Source: PubMed

Available online at www.sciencedirect.com
ScienceDirect
Biochemical and Biophysical Research Communications 349 (2006) 890–899
BBRC
www.elsevier.com/locate/ybbrc

NMR solution structure of BmK-βIT, an excitatory scorpion β-toxin without a 'hot spot' at the relevant position ☆

Xiaotian Tong [a,1], Jing Yao [b,1], Fahu He [a], Xiang Chen [a], Xunhai Zheng [a], Chang Xie [b], Gong Wu [a], Naixia Zhang [a], Jiuping Ding [b], Houming Wu [a,*]

[a] *State Key Laboratory of Bio-organic and Natural Products Chemistry, Shanghai Institute of Organic Chemistry, Chinese Academy of Sciences, Shanghai 200032, China*
[b] *Institute of Biochemistry and Biophysics, College of Life Science and Technology, Huazhong University of Science and Technology, Wuhan, Hubei 430074, China*

Received 28 July 2006
Available online 30 August 2006

Abstract

BmK-βIT (previously named as Bm32-VI in the literature), an excitatory scorpion β-toxin, is purified from the venom of the Chinese scorpion *Buthus martensii* Karsch. It features a primary sequence typical of the excitatory anti-insect toxins: two contiguous Cys residues (Cys37-Cys38) and a shifted location of the fourth disulfide bridges (Cys38-Cys64), and demonstrates bioactivity characteristic of the excitatory β-toxins. However, it is noteworthy that BmK-βIT is not conserved with a glutamate residue at the preceding position of the third Cys residue, and is the first example having a non-glutamate residue at the relevant position in the excitatory scorpion β-toxin subfamily. The 3D structure of BmK-βIT is determined with 2D NMR spectroscopy and molecular modeling. The solution structure of BmK-βIT is closely similar to those of BmK IT-AP and Bj-xtrIT, only distinct from the latter by lack of an α_0-helix. The surface functional patch comparison with those of BmK IT-AP and Bj-xtrIT reveals their striking similarity in the spatial arrangement. These results infer that the functional surface of β-toxins is composed of two binding regions and a functional site. The main binding site is consisted of hydrophobic residues surrounding the α_1-helix and its preceding loop, which is common to all β-type scorpion toxins affecting Na^+ channels. The second binding site, which determines the specificity of the toxin, locates at the C-terminus for excitatory insect β-toxin, while rests at the β-sheet and its linking loop for anti-mammal toxins. The functional site involved in the voltage sensor-trapping model, which characterizes the function of all β-toxins, is the negatively charged residue Glu15.

Keywords: BmK-βIT; Scorpion toxin; *Buthus martensii* Karsch; NMR; Solution structure

The scorpion venoms are a rich source of toxic peptides and have been shown to be composed of 28–76 amino acid residues. They interact selectively with the Na^+, K^+, Ca^{2+}, and Cl^- ion channels, which render them invaluable tools in probing the protein mapping of ion channels and clarifying the molecular mechanism involved in the signal transmission and channel gating. The long-chain neurotoxins containing 60–76 residues, stabilized by four disulfide bridges, act specifically on the voltage-dependent sodium channels of both vertebrates and insects [1–4]. These toxins have been divided into vertebrate toxins (including α and β) and insect toxins, according to the specificity and pharmacological activities [3–5]. Insecticidal toxins are further separated into groups of excitatory and depressant, which act together on sodium channel inactivation and activation, and resemble the mammalian β-toxin in their mode of action [6].

So far, several excitatory toxins have been identified, such as AaH IT1 from *Androctonus australis hector*,

☆ *Abbreviations:* 1D, one dimensional; 2D, two dimensional; 3D, three dimensional; DQF-COSY, double-quantum-filtered shift correlated spectroscopy; NMR, nuclear magnetic resonance; NOESY, nuclear overhauser enhancement spectroscopy; RMSD, root mean square deviation; TOCSY, total correlation spectroscopy.

* Corresponding author. Fax: +86 21 64166128.
E-mail address: hmwu@mail.sioc.ac.cn (H. Wu).

[1] These authors contributed equally to this work.

0006-291X/$ - see front matter © 2006 Elsevier Inc. All rights reserved.
doi:10.1016/j.bbrc.2006.08.131

LqqIT1 from *Leiurus quinquestriatus quinquestriatus*, and Bj-xtrIT from *Buthotus judaicus* (current name *Hottentotta judaica*). These toxins generate an immediate contraction paralysis of *Sarcophaga falculate* larvae, induce repetitive firing in the motor nerves by causing an increase of the peak sodium current a voltage-dependent slowing of sodium current inactivation [7–9]. The insect-specificity and prominent bioactivity of these toxins make them ideal candidates for potential application as biological insecticides in pest control, which attracts more and more interest among biologists and biochemists to better understand the structural basis for their functions. To date, of the excitatory toxins, only the 3D structures of Bj-xtrIT and BmK IT-AP have been determined by crystallographic studies [10,11]. Although the core structures of the two peptides are similar to those of other long-chain scorpion toxins active on sodium channels (α-helix anchored against a three-stranded β-sheet stabilized by three spatially conserved disulfide bonds), their unique structural feature with an additional extension of C-terminal region may be responsible for their special mode of action. More recently, it has been reported that the putative pharmacophore constituted by a number of non-polar and three charged amino acids clustered around the main α-helix motif and the C-tail of Bj-xtrIT is achieved by genetic modifications and structural analyses [12]. This discovery further boosts the interest in the study of insect-excitatory toxins.

As a part of our continuing structural investigations on scorpion toxins [13–21], we report here the purification, the characterization, and the solution structure of an excitatory toxin BmK-βIT (previously with a name of Bm32-VI). BmK-βIT has been reported as an excitatory β-toxin sensitive to insects in the literature [22]. Because of the limited amount available from natural resource, its 3D structure remains unknown. The primary sequence of BmK-βIT is distinct from other toxins in the β-excitatory toxin subfamily that a glutamate residue at the preceding position of the third Cys residue, which was assumed previously as a pharmacophore responsible for the β-type interaction mode, is not conserved in BmK-βIT. To determine the functional surface responsible for the interaction mode of β-excitatory toxin and gain insight into the relationship between the structure and bioactivity, the solution structure of the toxin has been determined and the results are reported in this article.

Materials and methods

Materials. Scorpions of the species *Buthus martensi* Karsch were collected from local culture farms in Henan province, China. The crude venom was obtained by electrically stimulating of the telson of scorpion. Acetonitrile was of spectroscopic grade. Other chemical reagents were of analytical reagent grade. Trifluoroacetic acid (TFA) was purchased from Merk. D_2O and DCl were obtained from Sigma. NaOD was available from Aldrich Chemical Company.

Sample preparation and chemical characterization. The peptide was isolated and purified using the same procedure as described previously [23]. The further separation of fraction III-2 was performed on Sephadex G-50 column, which was equilibrated and eluted with the same buffer as previously mentioned. Fraction III-2-1 from Sephadex G-50 column was then purified by HPLC using a C_{18} column (5 μm, 4.6 × 250 mm, Alltech), eluted at a flow rate of 1 mL/min with a linear gradient from A (water containing 10% acetonitrile and 0.1% trifluoroacetic acid) to 55% B (acetonitrile containing 20% water and 0.1% trifluoroacetic acid), affording the peptide BmK-βIT (10 mg). The purity and molecular weight of the peptide were determined on a triple-stage quadruple mass spectrometer (Quattro VG, UK) equipped with an electrospray ion source. Amino acid analysis was performed on a Beckman 6300 apparatus after hydrolysis of the samples in 6 mol/L HCl under vacuum at 110 °C for 20 h. The N-terminal sequence of BmK-βIT was achieved by Edman degradation using a Beckman LF3200 Protein-Peptide sequencer.

NMR experiments. The peptide BmK-βIT was dissolved in H_2O/D_2O (90/10 v/v) or 100% D_2O, pH 4.8 (uncorrected for isotope effects, adjusted by adding 1 μL of dilute DCl or NaOD). The final concentration of BmK-βIT was about 2.0 mmol/L. The amide proton exchange rate was determined after lyophilization and dissolution in 100% D_2O.

All the NMR experiments were recorded at 303 K on a Varian unity Inova 600 spectrometer. Quadrature detection was employed in all experiments and the carrier frequency always maintained at the solvent resonance. Presaturation was used to suppress the water peak in all experiments. Two dimensional DQF-COSY, TOCSY, and NOESY spectra were achieved in phase-sensitive mode by using the time-proportional phase incrementation method. All 2D-NMR spectra were recorded with 4 K data points in t_2 dimension and 512 data points in t_1 dimension. The TOCSY spectra were recorded using the MLEV-17 pulse sequence with mixing time of 30, 80, and 120 ms. The NOESY spectra were acquired using mixing time of 100, 150, 200, and 300 ms, respectively. A shifted sine window function and zero filling were applied prior to Fourier transformation. To determine slowly exchanging protons, a series of 1D spectra were recorded at 303 K during the first 2 h after the sample was dissolved in D_2O.

All experimental data were acquired and processed using Vnmr 6.1B program on a SUN Sparc station computer. The processed data were analyzed with XEASY for NMR spectra visualization, peak picking, and peak-integration on a Silicon Graphics Indigo R 5000 computer.

Experimental constraints and structure calculation. Distance constraints were obtained from the NOESY (150 and 200 ms) spectra acquired in H_2O, additional constraints were from the NOESY spectra in D_2O. Dihedral angle constraints were derived from $^3J_{HNH\alpha}$ coupling constants, which were obtained by analyses of 1D ^{1}H NMR spectrum. In the latter part of structure calculation, hydrogen-bond constraints (revealed by H–D exchange spectra) and the constraints derived from four disulfide bridges (Cys16-Cys37, Cys22-Cys42, Cys26-Cys44, and Cys38-Cys64) were added, where the presence of those constraints was determined on the basis of the geometry of the backbone in the early stage of the calculation. Distance geometry calculations were performed with the target function program DYANA on a Silicon Graphic Indigo II computer. The 35 structures with the lowest constraint violations were subjected to restrained energy minimization (REM) performed with the AMBER 5.0 package. Twenty best conformers with the lowest energy were used to represent the solution conformation of BmK-βIT. The program PROCHECK_NMR was used to evaluate the NMR structures of BmK-βIT. In addition, 3D conformations were produced with MOLMOL program for visual comparison of the structures on a Silicon Graphic Indigo II computer. For pairs of conformers, RMSD values for various subsets of atoms were calculated.

Results

Purification and characterization

The peptide BmK-βIT was purified from the crude venom of Chinese scorpion *Buthus martensii* Karsch by using the procedure as mentioned above [23]. The toxin-containing fraction III-2 from the Mono S cation exchange column

was further submitted to two-step purification of Sephadex G-50 column and HPLC, leading to the peptide BmK-βIT (10 mg) (Fig. 1A and B). The ESI-MS spectrum of the protein is shown in Fig. 1C, which gave a single peak at 7634 ($[M + H]^+$). The result of amino acid analysis of the toxin BmK-βIT is listed in Table 1. The N-terminal sequence of BmK-βIT determined by Edman degradation was KKNGYAVDSSGKVS. The complete sequence of BmK-βIT was determined by the mass data and the database searching. It was further supported by NMR experiments .

NMR assignments

The identification of amino acid spin systems and the sequential assignment were done using the standard strategy described by Wüthrich [24].

The spin systems of BmK-βIT were identified on the basis of DQF-COSY and TOCSY spectra recorded with various mixing times in H_2O and D_2O at pH 4.8 and 303 K. The fingerprint region of the DQF-COSY spectra recorded in H_2O showed most of HN–H_α cross peaks expected and then the TOCSY spectra were used to correlate the HN–H_α cross peaks with their side chain spin systems for each residue. The spin systems of tyrosine and phenylalanine were assigned by the presence of intraresidual NOE cross peaks of H_δ–H_β and H_δ–H_α. Likewise, spin systems of one Gln and five Asn were determined by NOE correlations of NH_δ to H_β and NH_ε to H_γ, appearing only in H_2O spectra. Complete identification of amino acid residues for BmK-βIT was achieved at the stage of sequence-specific assignments.

The spin systems of BmK-βIT were connected in sequence by virtue of $d_{\alpha N}$, d_{NN}, and $d_{\beta N}$ connectivities in well-dispersed NOESY spectra. Sequential NOE connectivities were observed for all residues of the protein, except for Lys2/Asn3 and Ser14/Glu15. The sequential and medium-range NOE contacts as well as $^3J_{HNH\alpha}$ coupling constants and amide proton exchange data are summarized in Fig. 3.

Secondary structure

Secondary structure elements of BmK-βIT were identified using the unique NOE cross peaks, $^3J_{HNH\alpha}$ coupling constants, and slowly exchanged amide protons [24]. For example, helical conformations are characterized by the strong continuous strong $d_{NN}(i, i+1)$ and medium $d_{\alpha N}(i, i+1)$, as well as small $^3J_{HNH\alpha}$ (<7.0 Hz) coupling constants. On the other hand, β-sheets are characteristic of strong $d_{\alpha N}(i, i+1)$ connectivities and large $^3J_{HNH\alpha}$ (>9.0 Hz) coupling constants. In the peptide BmK-βIT, a 3-turn α_1-helix and a 1.5-turn α_2-helix at C-terminus were observed formed by residues Asn19-Val29 and Asp58-Tyr63, respectively. A three-stranded anti-parallel β-sheet (for residues Asn3-Tyr5, Ser34-Cys38, and Ser41-Phe45) was inferred from a network of long-range backbone–

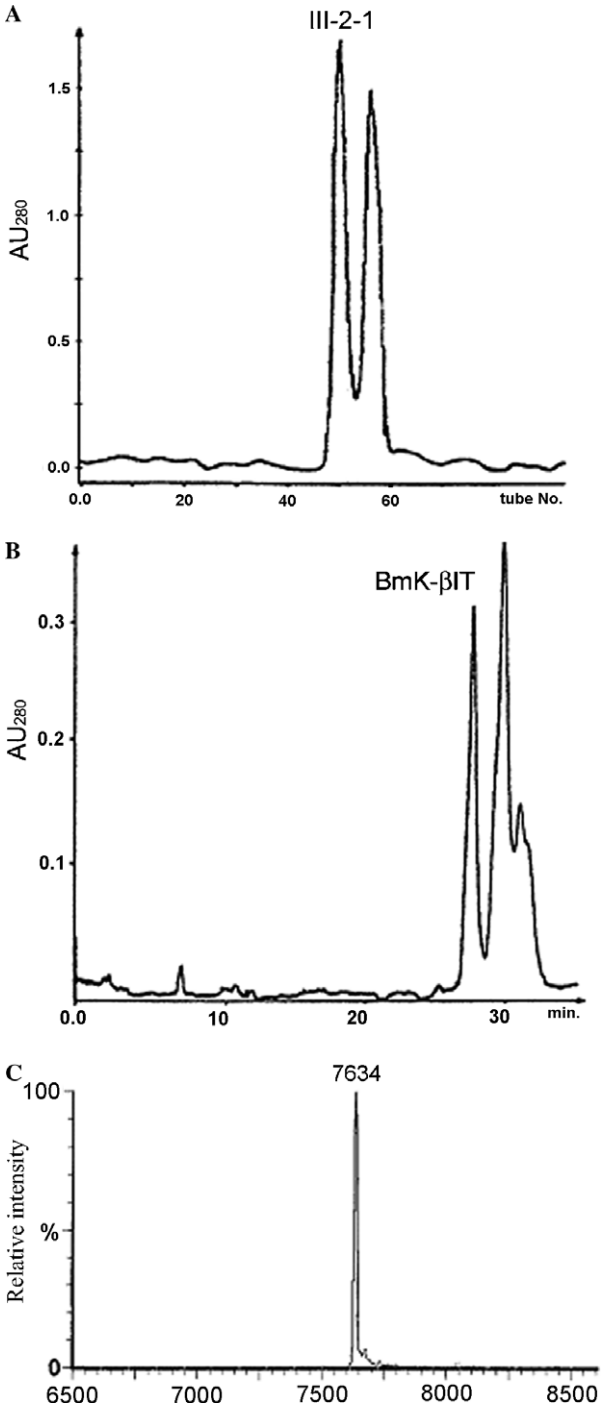

Fig. 1. Isolation and purification of BmK-βIT. (A) Gel-filtration chromatography of fraction III-2 on a Sephadex G-50 column. (B) Final step of purification of BmK-βIT on a C_{18} column, eluted with a linear gradient from solution A (water containing 10% acetonitrile and 0.1% trifluoroacetic acid) to 55% solution B (acetonitrile containing 20% water and 0.1% trifluoroacetic acid). (C) ESI-MS spectrum of BmK-βIT.

backbone interactions ($d_{\alpha N}$, $d_{\alpha\alpha}$, and d_{NN} NOEs) and slowly exchanging amide protons.

Tight turns are characterized by two medium-to-strong consecutive $d_{NN}(i, i+1)$ cross peaks and distinct patterns of J coupling constants for each type turn. Two type-I

Table 1
Amino acid compositions of BmK-βIT

Amino acid	No. of residues
Asx	11.34 (11)
Thr	2.88 (3)
Ser	5.70 (6)
Glx	2.36 (2)
Gly	3.95 (4)
Ala	4.18 (4)
Val	4.62 (5)
Ile	3.60 (4)
Leu	6.40 (6)
Tyr	6.51 (7)
Phe	1.42 (1)
Lys	7.90 (8)
Cys-Cys	3.23 (4)
MW (calculated)	7633.8
MW (experimental)	7634.0

turns (Leu38-Ser41 and Lys28-Tyr31) and one regular five-residue turn (Val8-Gly12) were identified by characteristic NOE patterns (Fig. 3).

Deviations of chemical shifts of H_α protons from their random coil values were suggested to be a useful indicator of secondary structure [25,26]. Commonly, negative deviations for a series of continuous residues are typical of helical structures, whereas positive deviations are indicative of β-sheet. In BmK-βIT, the values of deviation are in good agreement with the helixes (Asn19-Val29 and Asp58-Tyr63) and β-sheet (Asn3-Tyr5, Ser34-Cys38, and Ser41-Phe45) (see Fig. 3). These data further confirmed the deduction for the secondary structure of BmK-βIT.

Structure determination

The input for the distance geometry calculations with the program DYANA consisted of upper distance limits derived from NOESY (mixing time 150 and 200 ms) cross-peak intensities using the program CALIBA, and dihedral angle constraints obtained from an initial interpretation of the vicinal coupling constants $^3J_{HNH\alpha}$. For the calibration of proton–proton distance limits (r versus the cross-peak intensities), the dependence of $1/r^6$ was used for all protons. The calibration curves were refined based on plotting cross peak volume versus average proton–proton distance according to the preliminary structures. A total of 814 distance constraints were used (346 intraresidual, 202 sequential, 85 medium-range, and 181 long-range NOEs). 27 ϕ angle constraints ($-55 \pm 15°$ for $^3J_{HNH\alpha} < 7.0$ Hz and $-125 \pm 45°$ for $^3J_{HNH\alpha} > 9.0$ Hz) were used for structure calculation. In addition, 12 constraints were added for the four-disulfide bonds (3 per bond). Sixteen slow-exchanging amide protons were determined from the H–D exchanging experiments and were used to generate hydrogen bond constraints. For each hydrogen bond, two limit restraints were used between the NH—O (0.22 nm) and the N—O (0.32 nm) atom pairs. In addition, the program GLOMSA was used to obtain four stereo-specific assignments of methylenes and two isopropyl methyls on the basis of the preliminary structures. Totally, 885 constraints (average 12.8 constraints per residue) were obtained and used in the structure calculations for BmK-βIT.

Starting from 200 random structures, 35 preliminary structures with lowest target functions resulted from distance geometry calculations were subjected to simulated annealing and restrained energy minimization (REM) using the SANDER module of the AMBER 5.0 package. A cutoff radius of 0.8 nm for non-bonded interactions, with a residue-based pair-list routine, was used in all calculations. The force constants for distance restraints in REM were 500 kJ mol^{-1} nm^{-2}. Energy minimization was performed using a combination of steepest descent and conjugate gradient algorithms with a gradient convergence norm

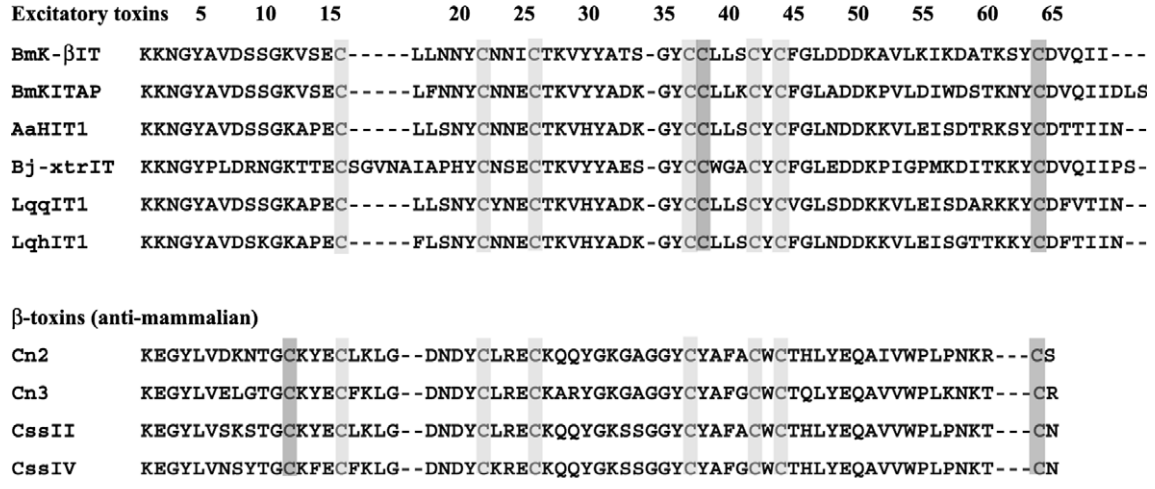

Fig. 2. Sequence alignments of BmK-βIT with selected excitatory toxins and β-toxins. Sequences are aligned according to the cysteine frame. Dashes indicate gaps. Numbers are labeled with respect to the sequence of BmK-βIT. The cysteine (highlighted with black gray box) cross-linked to the last cysteine is dramatically shifted from position 12 in β-toxins to 38 in BmK-βIT and in all excitatory toxins.

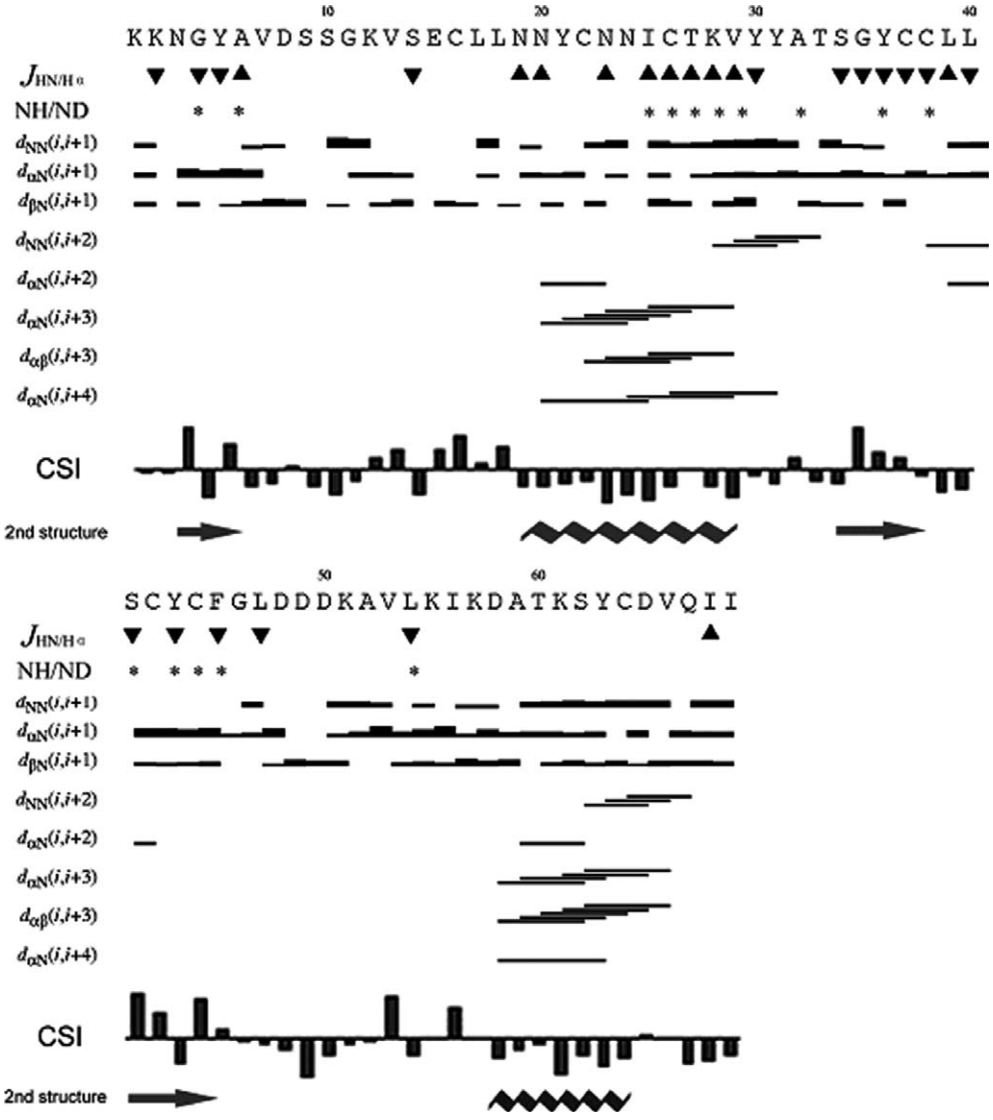

Fig. 3. Summary of NOE connectivities, *J*-coupling constants $^3J_{HN/H\alpha}$, the amide proton exchange rate, and $C^{\alpha}H$ chemical shift index. The thickness of the bar indicates the intensity of NOEs. Asterisks represent the NH protons in slowly exchanging. *J*-coupling constants $^3J_{HN/H\alpha}$ are smaller than 7.0 Hz (▲) and larger than 9.0 Hz (▼). Positive and negative bars in the chemical shift index (CSI) indicate the $C^{\alpha}H$ protons downfield-shifted and upfield-shifted, respectively, as compared with the $C^{\alpha}H$ proton chemical shifts in random-coil. The locations of the 2nd structures found in BmK-βIT are also indicated.

of less than 10^{-4} kJ mol^{-1} nm^{-1}. After energy minimization with AMBER, the 20 best DYANA conformers with the lowest energy are used to represent the solution conformation of BmK-βIT.

Solution structure of BmK-βIT

Fig. 4A represents the superposition of the polypeptide backbones of 20 best conformers. No NOE violations larger than 0.20 Å and no angle violations exceeding 5° can be found. The overall agreement among individual conformers is indicated by global root-mean square deviations (RMSD). The final set of 20 structures displays an overall RMSD of 1.15 Å for the backbone atoms and 1.76 Å for all heavy atoms. The RMSD values for the backbone atoms and heavy atoms are decreased to 0.56 Å and 1.15 Å, when the calculation is restricted to the residues forming the secondary structures. Analysis of the ensemble of 20 structures using PROCHECK_NMR reveals that 99.3% of the residues lie in the most favored and allowed regions of the Ramachandran ϕ, ψ dihedral angle plot. The structural statistics for 20 conformers of the toxin are summarized in Table 2.

The structure of BmK-βIT with the lowest energy is shown in Fig. 4B. The first 54 residues are compacted with well-defined core consisting of an α-helix linked to a three-stranded β-sheet and a long loop extending out from the core in the N-terminal region. Residues 3–5 (strand I), 34–38 (strand II), and 41–45 (strand III) form the anti-parallel three-stranded β-sheet, meanwhile, residues 19–29 fold into the α-helix. The α-helix is linked to the β-sheet by two disulfide bridges (Cys22-Cys42 and Cys26-Cys44) that are

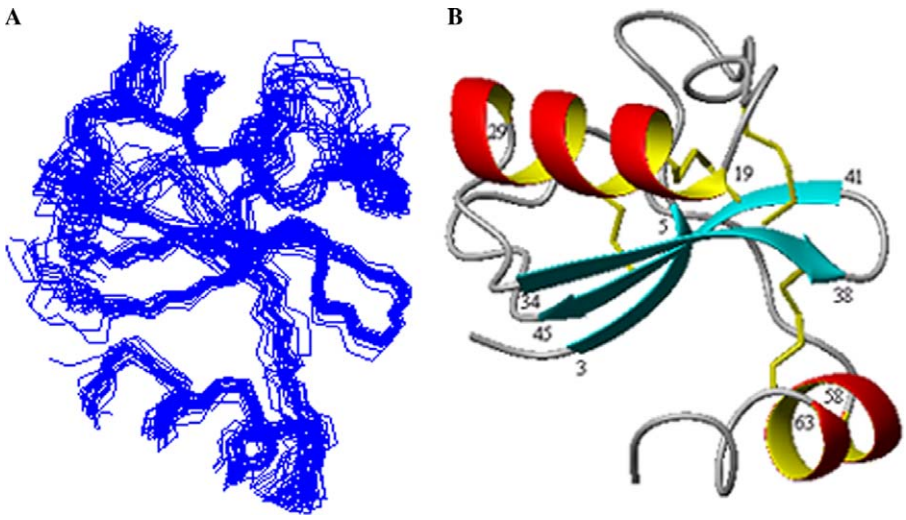

Fig. 4. Structure of BmK-βIT. (A) Backbone superimposition of the best 20 structures of BmK-βIT. (B) MOLMOL representation of the structure of BmK-βIT with the lowest energy. Beginning and ending residues of each secondary structural element are labeled according to protein sequence. Nt and Ct indicate N-terminus and C-terminus, respectively.

Table 2
Structural statistics for BmK-βIT

DYANA (35 best structures)			
Target function (Å^2)	0.11 ± 0.0235	Average no. of angle restraint violations > 5°/structure	0.0
Average no. of upper restraint violations > 0.2 Å/structure	0.0	Max violation (deg)	0.04
Max violation (Å)	0.16		
AMBER (20 best structures)			
Total energy (kcal/mol)	-983.81 ± 26.02	Rmsd from mean coordinates	
Bond energy (kcal/mol)	14.02 ± 0.56	All backbone atoms (Å)	1.15
Angle energy (kcal/mol)	80.64 ± 5.31	All heavy atoms (Å)	1.76
Dihed energy (kcal/mol)	129.09 ± 7.29	Structural analysis (%)	
Vdwaals energy (kcal/mol)	-344.71 ± 8.58	Residues in most favored regions	62.4
Eel energy (kcal/mol)	-2013.65 ± 39.50	Residues in allowed regions	32.9
H bond energy (kcal/mol)	-27.28 ± 1.65	Residues in generously allowed regions	4.0
Constraint energy (kcal/mol)	10.80 ± 1.75	Residues in disallowed regions	0.7

conserved in all long-chain scorpion toxins. The helix and the second β-strand are connected by a type-I turn formed by residues Tyr28-Thr31. A hairpin turn (Cys38-Ser41) linking the second and third strands is determined to be type-I β-turn on the basis of characteristic NOE patterns.

The C-terminal segment of BmK-βIT involving residues Lys55-Ile69 adopts a well-defined conformation. This part of the molecule forms an additional α-helix spanning residues Asp58-Tyr63, and residues following the helix adopt a coil topology, which is indicated by a series of medium-to-strong $d_{NN}(i,i+1)$ and $d_{\alpha N}(i,i+1)$ NOE cross peaks. The conformation of C-terminal region is stabilized by the fourth disulfide bridge (Cys38-Cys64) and by intra-molecular contacts between the Asp65-Ile69 segment and the core structure of the protein, which are revealed by several long-range NOEs between them. Additionally, the long-range hydrogen bond from Leu54 N to Tyr5 O, inferred from NMR structure, further contributes to the stability of the C-terminal region.

Comparison of BmK-βIT to other scorpion toxins

To better understand the molecular basis of the interaction between the toxin and Na^+ channels, we compared the 3D structure of BmK-βIT with those of typical β-toxins. Figs. 5A and B display the best-fit superposition of the backbone of BmK-βIT with the insect-specific excitatory toxins BmK IT-AP and Bj-xtrIT, whose structures were determined by X-ray crystallography [10,11]. Superposition of Cα atoms of BmK-βIT and BmK IT-AP (Fig. 5A) shows that two toxins have a very similar overall fold, and the root mean sequence deviation (RMSD) is 1.25 Å. Meanwhile, the structural comparison of BmK-βIT and Bj-xtrIT (Fig. 5B) indicates that the secondary structures in both toxins are identical except for the extra α_0 helix formed by residues 19–22 in toxin Bj-xtrIT. The root mean sequence deviation (RMSD) for the corresponding residues in segments Asn3-Asp8, Asn20-Val29, Ser34-Phe45, and Asp56-Cys64 is 1.09 Å upon best fitting of backbone con-

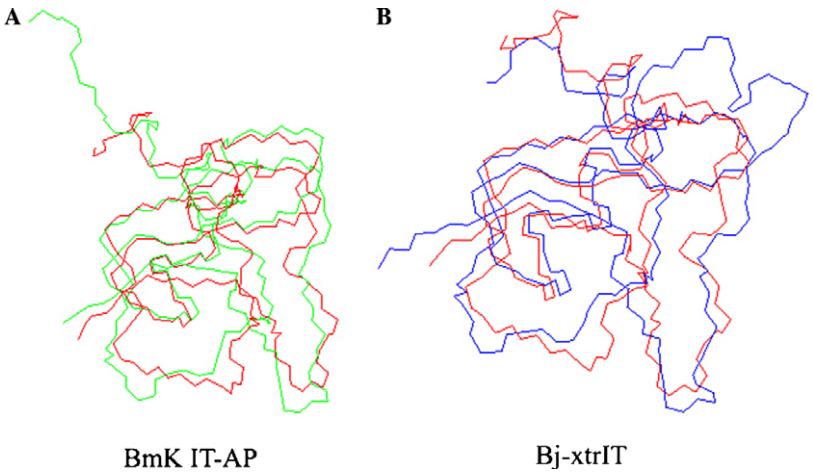

Fig. 5. Best fit superposition of backbone structures of BmK-βIT (red) and BmK IT-AP (green, A) and Bj-xtrIT (blue, B). The coordinates were obtained from PDB: 1WWN, 1T0Z, and 1BCG, respectively.

formation of BmK-βIT with Bj-xtrIT. The major differences in conformations among the three excitatory toxins locate at the loops connecting the secondary structure elements. Furthermore, the superposition of the 3D structure of BmK-βIT, BmK IT-AP, and Bj-xtrIT reveals close fit of the relevant residues in each functional patch among these toxins. When the residue Glu15 of these three toxins is superposed, the residue Tyr21, Ile25 and Val29 in BmK-βIT stand for the residue Tyr21, Glu25 and Val29 in BmK IT-AP and Tyr26, Glu30, Val34 in Bj-xtrIT as the main binding site. Meanwhile the stretch of hydrophobic residues, Val66, Gln67, Ile68, and Ile69 both on the C-tail of BmK-βIT and BmK IT-AP, is closely parallel to those residues (Val71, Gln72, Ile73, and Ile74) in Bj-xtrIT. Therefore, BmK-βIT can be referred to as a natural mutant of excitatory β-toxin BmK IT-AP and Bj-xtrIT for comparison.

Discussion

Physiological and primary features of BmK-βIT

BmK-βIT induces paralytical symptoms typical of insect contractive toxins: after a few seconds of uncoordinated motion, it fell on its dorsal side with violent trembling of its body and legs. The Ed_{50} on cockroach is 0.19 ng/mg, which is consistent with the value (0.18 ng/mg) on crickets reported in the literature [22]. These values are in the same toxicity range of an AaH IT1 sample (0.099 ng/mg insect) tested under the same conditions [27].

The electro-physiological properties of BmK-βIT have been well-characterized previously in the literature [22]. Under voltage-clamp conditions, BmK-βIT toxin induced (1) an increase of axonal excitability and (2) a resting depolarization together with a decrease of action potential amplitude. According to the literature, the increase of axonal excitability results from a shift to more negative values in voltage dependence of sodium channel activation. Increased Na^+ conductance at negative potential values is responsible for axonal hyper-excitability and the contractive paralysis of insect prey. Therefore, BmK-βIT demonstrates pharmacological characteristics of anti-insect excitatory scorpion β-toxins.

The sequential homology and the structure of BmK-βIT are compared with those of a few representative excitatory toxins, as well as anti-mammal scorpion β-toxins as shown in Fig. 2. Toxin BmK-βIT is highly homologous (identity of 80.6%) to toxin BmK IT-AP isolated from the same venom [28]. Meanwhile, the sequence homology of BmK-βIT with AaH-IT1 is 78.6%. In addition, the sequence alignments show that BmK-βIT has the feature of primary structure typical for the excitatory insect toxins: two contiguous Cys residues (Cys37-Cys38) and a shifted location of the fourth disulfide bridges (Cys38-Cys64). These structural features in common should place these peptides in the same group of insect selective excitatory sodium channel toxins.

On the other hand, BmK-βIT is distinct from other β-toxins in the primary sequence. For all β-toxin found to date, a glutamate residue is conserved at the preceding position of the third Cys residue for all excitatory insect β-toxins, or a glutamate residue is conserved at the preceding position of fourth Cys residue for other β-toxins as shown in Fig. 2. In 3D structure, this Glu residue is spatially conserved and located at the middle of the α_1 helix with its side chain extruding to the solvents. So far, a putative "hot-spot" with the Glu residue as the center flanked by two hydrophobic residues has been identified as a pharmacophore, which is responsible for the affinity to the Na^+ channels [12]. As compared with typical β-excitatory toxins and other β-toxins, the most unique in the primary sequence of BmK-βIT is that the residue at the relevant position is a hydrophobic Ile residue instead of a Glu residue. Thus, BmK-βIT is the first example of β-excitatory

insect toxins with a non-glutamate residue at the relevant position in nature. Furthermore, analysis of the solvent-exposed surface of BmK-βIT indicated that BmK-βIT has no such negatively charged "hot-spot" on the α_1 helix and preceding loop of the molecule as found in other β-toxins (refer to latter discussion). Therefore, a question is raised that why BmK-βIT toxin lack of a "hot-spot" usually found in other β-toxins demonstrates bioactivity typical for the excitatory β-toxins and what should be responsible for the affinity and binding with the Na^+ channels.

Implicated functional surface of BmK-βIT

The functional surface dissection of β-toxins has been well-documented using site-directed mutational analysis and mainly focused on the excitatory insect toxin Bj-xtrIT, as well as on the mammal-sensitive toxin Css4 in the literature [9,10,12,29,30]. The results have revealed that the putative functional surface of all β-toxins composed of: (1) a cluster of residues associated with the α-helix including a putative 'hot spot', referred to as the 'pharmacophore' of β-toxins. (2) A hydrophobic cluster, which is likely to confer the specificity, formed by a stretch of hydrophobic residues on the C-tail (for insect Na^+ channels) or associated mainly with the β2 and β3 strands (for mammalian Na^+ channels). (3) A negatively charged residue (Glu-15) involved in voltage sensor trapping.

The toxicity (ED_{50}) of BmK-βIT on crickets is 0.18 ng/mg, which is about 2 times potential than that (0.49 ng/mg) of BmK IT-AP [22] and is comparable to that (0.14 ng/mg on blowfly larvae) of Bj-xtrIT [29]. In addition, Izhar et al., demonstrated that the substitution of the acidic residue Glu30 of Bj-xtrIT by Leu reduced the toxicity 29-fold, whereas a conserved substitution to Asp had a smaller effect (8.3-fold) [29]. In the former case, the hydrophobic Leu residue may have suffered from

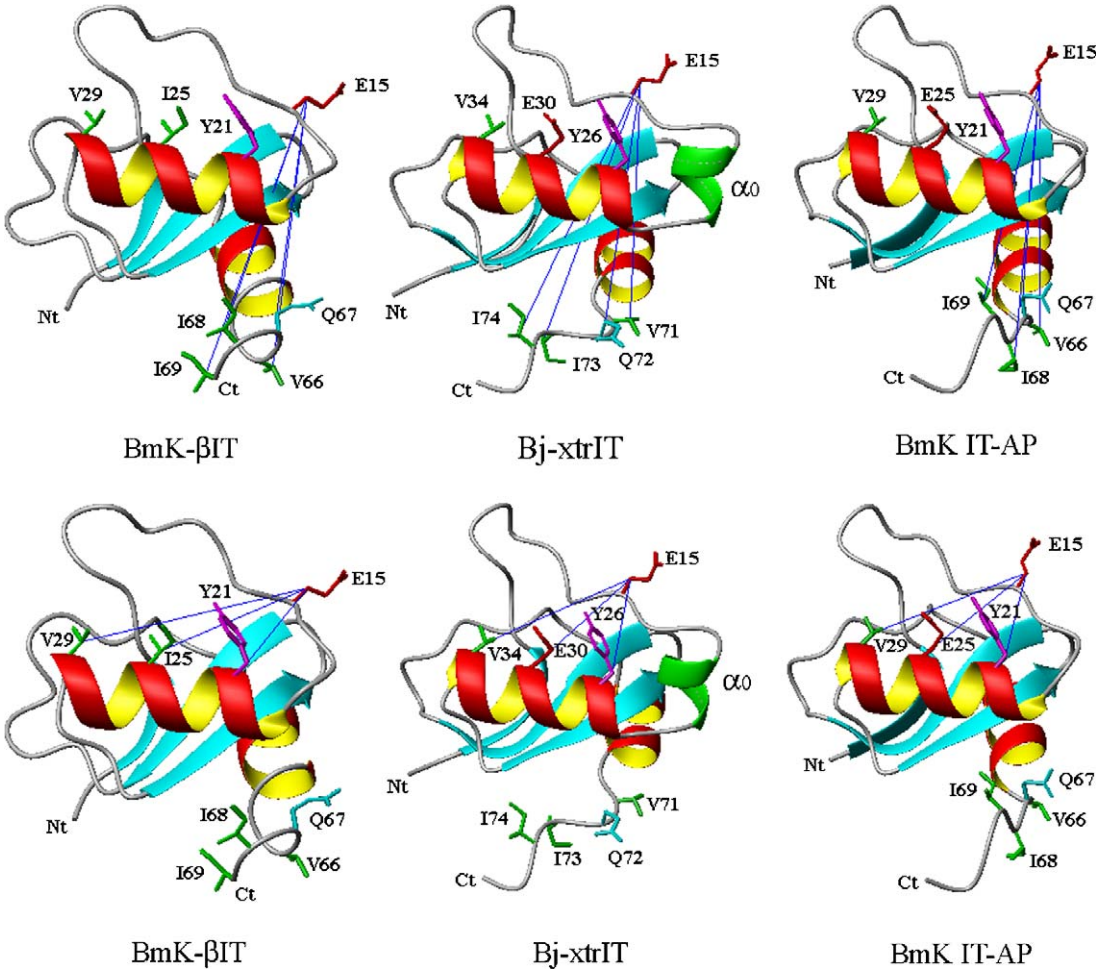

Fig. 6. Residues involved in the functional surface of BmK-βIT, Bj-xtrIT, and BmK IT-AP responsible for their anti-insect activity. Nt and Ct indicate N-terminus and C-terminus, respectively. The distances between the Cβ atoms of bioactive residues that determine the specificity (in BmK-βIT and Bj-xtrIT: V66, Q67, I68, I69, in Bj-xtrIT: V71, Q72, I73, I74) to the Cβ atom of the key residue Glu15 conserved in excitatory toxins are 21.10 ± 2.18, 21.34 ± 1.59, and 21.17 ± 2.44 Å in BmK-βIT, Bj-xtrIT, and BmK IT-AP, respectively. And the distances between the ones of functional residues that suggested to be responsible for binding affinity to sodium channels (in BmK-βIT: Y21, I25, V29, in Bj-xtrIT: Y26, E30, V34, in BmK IT-AP: Y21, E25, V29) to the one of the key residues Glu15 are 12.33 ± 2.65, 11.47 ± 1.58, and 11.77 ± 2.00 Å, respectively. The distances among the three domains that are suggested to constitute the functional surface for anti-insects in excitatory toxins are in the same range.

unfavorable contact due to hindered germinal methyl at the terminus of the side chain. In the latter case the Asp residue has no favorable electrostatic contribution to the interaction with its target channel due to its too short side chain to form a salt bridge with a basic residue at the counterpart, nor hydrophobic contact due to its polar property. In BmK-βIT, the hydrophobic Ile residue may have hydrophobic interaction with the side chain of the counterpart residue at relevant position and avoid the unfavorable contact due to its specific side chain pattern. Thus the better biological activity than those of Bj-xtrIT mutant E30L and E30D seems reasonable. Currently, there are no toxicity data of Bj-xtrIT mutant E30I and the detailed structural information on the counterpart in the channel to confirm this proposition, which remains future study.

On the other hand, Cohen et al. pointed out that scorpion β-toxins demonstrated the similarity in the spatial arrangement of the functional surface [30]. To validate the striking similarity of the spatial functional surface arrangements in these toxins, distances between the functional surfaces were compared among these toxins. As shown in Fig. 6, the distances between the β-C atoms of bioactive residues that determine the specificity (in BmK-βIT and BmK IT-AP: V66, Q67, I68, I69, in Bj-xtrIT: V71, Q72, I73, I74) to the Cβ atom of the key residue Glu15 conserved in excitatory toxins are 21.10 ± 2.18, 21.34 ± 1.59, and 21.17 ± 2.44 Å in BmK-βIT, Bj-xtrIT, and BmK IT-AP, respectively. And the distances between the Cβ atoms of functional residues that suggested to be responsible for binding affinity to sodium channels (in BmK-βIT: Y21, I25, V29, in Bj-xtrIT: Y26, E30, V34, in BmK IT-AP: Y21, E25, V29) to the Cβ atoms of the key residue Glu15 are 12.33 ± 2.65, 11.47 ± 1.58, and 11.77 ± 2.00 Å, respectively. The distances among the three domains that are suggested to constitute the functional surface for anti-insects in excitatory toxins are in the same range.

It is noteworthy that all these sites located at the spatial fixed positions of the molecule, particularly associated with the Cys-Cys bridges. The central residue of the main binding patch Glu30 (or Ile25 for BmK-βIT) locates at the middle of the helix between two Cys bridges (Cys22-Cys42 and Cys26-Cys44), which link the α_1-helix and the β-sheet to form the core of the molecule. Residue Glu15 rests at the preceding position of the Cys16-Cys37 bridge, which connect the preceding loop of the α-helix to the β-sheet. The C-terminus is anchored by the fourth disulfide bridge and supported by intra-molecular contacts between the C-tail and the α/β-core of the molecule. This kind arrangement of the molecule makes all β-toxins having the striking similarity and geometric rigidity in the spatial functional surface arrangements, which is necessary for the interaction with their target channels.

Recently, it has been reported that modifications of Glu15 in Bj-xtrIT only affect their bioactivity but have minor effect on binding affinity, whereas substitutions of Glu30 impair both toxicity and binding [12,29]. From these reasons, it has been assumed that Glu15 is the key residue in the excitatory toxins that interacts with their receptor through direct electrostatic interactions, while the 'hot spot' previously suggested as the "pharmacophore" together with the hydrophobic residues (Tyr and Val in excitatory toxins) mainly contributes to the binding affinity to its receptor and the C-terminal segment determines the specificity to insects.

In summary, the functional surface of β-toxins is composed of two binding regions and a functional site. The main binding site consists of hydrophobic residues surrounding the α_1-helix and its preceding loop with a "hot spot" as the center in most cases (but not in all cases, like as the present case), which is common to all β-type scorpion toxins affecting Na^+ channels. The second binding site, which determines the specificity of the toxin, locates at the C-terminus for excitatory insect β-toxin, while it rests at the β-sheet and its linking loop for anti-mammal toxins. The functional site or "the pharmacophore" involved in the voltage sensor-trapping model, which characterizes the function of all β-toxins, should be the negatively charged residue Glu15.

Data bank accession number

The atomic coordinates of the 20 energy-minimized conformers used to represent the solution structure of BmK-βIT have been deposited in the Protein Data Bank, together with the input of conformational restrains used for the structure calculation under Accession No. 1WWN.

Acknowledgments

This project was supported by the National Science Foundation of China (Grant No. 20132030), and Chinese Academy of Sciences (Grant No. KGCX2-SW-213-05). The authors thank the Institute of Molecular Biology and Biophysics, ETH-Hönggerberg Zürich, Switzerland, for giving the programs DYANA (version 1.5) and XEASY. We are grateful to Prof. Bertini of Florence University, Italy, for giving the program CALIBA and Prof. James W. Caldwell of California University, USA, for the program AMBER.

Appendix A. Supplementary data

Supplementary data associated with this article can be found, in the online version, at doi:10.1016/j.bbrc.2006.08.131.

References

[1] L.D. Possani, in: A.T. Tu (Ed.), Handbook of Natural Toxins, vol. 2, Marcel Dekker Inc., New York, 1984, pp. 513–550.
[2] D. Gordon, P. Savarin, M. Gurevitz, S. Zinn-Justin, Functional anatomy of scorpion toxins affecting sodium channels, J. Toxicol. Toxin Rev. 17 (1998) 131–159.

[3] L.D. Possani, B. Becerril, M. Delepierre, J. Tytgat, Scorpion toxins specific for Na^+-channels, Eur. J. Biochem. 264 (1999) 287–300.
[4] C. Goudet, C.W. Chi, J. Tytgat, An overview of toxins and genes from the venom of the Asian scorpion *Buthus martensi* Karsch, Toxicon 40 (2002) 1239–1258.
[5] M.F. Martin-Eauclaire, F. Couraud, in: L.W. Chang, R.S. Dyer (Eds.), Handbook of Neurotoxicology, Marcel Dekker Inc., New York, 1995, pp. 683–716.
[6] E. Zlotkin, in: P. Lazarovici, Y. Gutman (Eds.), Toxins and Signal Transduction, Harwood Press, Amsterdam, 1997, pp. 95–117.
[7] M. Pelhate, E. Zlotkin, Actions of insect toxin and other toxins derived from the venom of the scorpion *Androctonus australis* on isolated giant axons of the cockroach (*Periplaneta americana*), J. Exp. Biol. 97 (1982) 67–77.
[8] E. Zlotkin, D. Kadouri, D. Gordon, M. Pelhate, M.F. Martin, H. Rochat, An excitatory and a depressant insect toxin from scorpion venom both affect sodium conductance and possess a common binding site, Arch. Biochem. Biophys. 240 (1985) 877–887.
[9] O. Froy, N. Zilberberg, D. Gordon, M. Turkov, N. Gilles, M. Stankiewicz, M. Pelhate, E. Loret, D.A. Oren, B. Shaanan, M. Gurevitz, The putative bioactive surface of insect-selective scorpion excitatory neurotoxins, J. Biol. Chem. 274 (1999) 5769–5776.
[10] D.A. Oren, O. Froy, E. Amit, N. Kleinberger-Doron, M. Gurevitz, B. Shaanan, An excitatory scorpion toxin with a distinctive feature: an additional alpha helix at the C terminus and its implications for interaction with insect sodium channels, Structure 6 (1998) 1095–1103.
[11] C. Li, R.J. Guan, Y. Xiang, Y. Zhang, D.C. Wang, Structure of an excitatory insect-specific toxin with an analgesic effect on mammals from the scorpion *Buthus martensii* Karsch, Acta Crystallogr. Sect. D 61 (2005) 14–21.
[12] L. Cohen, I. Karbat, N. Gilles, O. Froy, G. Corzo, R. Angelovici, D. Gordon, M. Gurevitz, Dissection of the functional surface of an anti-insect excitatory toxin illuminates a putative "hot spot" common to all scorpion beta-toxins affecting Na^+ channels, J. Biol. Chem. 279 (2004) 8206–8211.
[13] H.M. Wu, G. Wu, X.L. Huang, F.H. He, S.K. Jiang, Purification, characterization and structural study of the neuro-peptide from scorpion *Buthus martensi* Karsch, Pure Appl. Chem. 71 (1999) 1157–1162.
[14] G. Wu, Y.M. Li, D.S. Wei, F.H. He, S.K. Jiang, G.Y. Hu, H.M. Wu, Solution structure of BmP01 from the venom of scorpion *Buthus martensii* Karsch, Biochem. Biophys. Res. Commun. 276 (2000) 1148–1154.
[15] F.H. He, Y.M. Li, G. Wu, C.Y. Cao, H.M. Wu, Three-dimensional structure BmP03 from the venom of scorpion *Buthus martensi* Karsch, Acta Chim.. Sin. 58 (2000) 850–855.
[16] M.H. Li, N.X. Zhang, X.Q. Chen, G. Wu, H.M. Wu, G.Y. Hu, BmKK4, a novel toxin from the venom of Asian scorpion *Buthus martensi* Karsch, inhibits potassium currents in rat hippocampal neurons in vitro, Toxicon 42 (2003) 199–205.
[17] N.X. Zhang, G. Wu, Y.F. Wang, Z.H. Wang, C.L. Feng, H.M. Wu, Purification and primary structure of a toxin-like peptide BmK622 from the venom of Chinese scorpion *Buthus martensi* Karsch, Acta Chim. Sin. 61 (2003) 630–634.
[18] N.X. Zhang, M.H. Li, X. Chen, Y.F. Wang, G. Wu, G.Y. Hu, H.M. Wu, Solution structure of BmKK2, a new potassium channel blocker from the venom of Chinese scorpion *Buthus martensi* Karsch, Proteins 55 (2004) 835–845.
[19] N.X. Zhang, X. Chen, M.H. Li, C.Y. Cao, Y.F. Wang, G. Wu, G.Y. Hu, H.M. Wu, Solution structure of BmKK4, the first member of subfamily alpha-KTx 17 of scorpion toxins, Biochemistry 43 (2004) 12469–12476.
[20] Y.F. Wang, X. Chen, N.X. Zhang, G. Wu, H.M. Wu, The solution structure of BmTx3B, a member of the scorpion toxin subfamily alpha-KTx 16, Proteins 58 (2005) 489–497.
[21] J. Yao, X. Chen, H. Li, Y. Zhou, L.J. Yao, G. Wu, X.K. Chen, N.X. Zhang, Z. Zhou, T. Xu, H.M. Wu, J.P. Ding, BmP09, a "long chain" scorpion peptide blocker of BK channels, J. Biol. Chem. 280 (2005) 14819–14828.
[22] P. Escoubas, M. Stankiewicz, T. Takaoka, M. Pelhate, R. Romi-Lebrun, F.Q. Wu, T. Nakajima, Sequence and electrophysiological characterization of two insect-selective excitatory toxins from the venom of the Chinese scorpion *Buthus martensi* Karsch, FEBS Lett. 483 (2000) 175–180.
[23] G. Wu, D.S. Wei, F.H. He, G.Y. Hu, H.M. Wu, A K^+ channel-blocking peptide from venom of Chinese scorpion *Buthus martensi* Karsch, Zhongguo Yao Li Xue Bao 19 (1998) 317–321.
[24] K. Wüthrich, in: NMR of Proteins and Nucleic Acid, Wiley, New York, 1986, p. 292.
[25] D.S. Wishart, B.D. Sykes, F.M. Richards, Relationship between nuclear magnetic resonance chemical shift and protein secondary structure, J. Mol. Biol. 222 (1991) 311–333.
[26] D.S. Wishart, B.D. Sykes, F.M. Richards, The chemical shift index: a fast and simple method for the assignment of protein secondary structure through NMR spectroscopy, Biochemistry 31 (1992) 1647–1651.
[27] E.P. Loret, P. Mansuelle, H. Rochat, C. Granier, Neurotoxins active on insects: amino acid sequences, chemical modifications, and secondary structure estimation by circular dichroism of toxins from the scorpion *Androctonus australis* Hector, Biochemistry 29 (1990) 1492–1501.
[28] Y.M. Xiong, Z.D. Lan, M. Wang, B. Liu, X.Q. Liu, H. Fei, L.G. Xu, Q.C. Xia, C.G. Wang, D.C. Wang, C.W. Chi, Molecular characterization of a new excitatory insect neurotoxin with an analgesic effect on mice from the scorpion *Buthus martensi* Karsch, Toxicon 37 (1999) 1165–1180.
[29] I. Karbat, L. Cohen, N. Gilles, D. Gordon, M. Gurevitz, Conversion of a scorpion toxin agonist into an antagonist highlights an acidic residue involved in voltage sensor trapping during activation of neuronal Na^+ channels, FASEB J. 18 (2004) 683–689.
[30] L. Cohen, I. Karbat, N. Gilles, N. Ilan, M. Benveniste, D. Gordon, M. Gurevitz, Common features in the functional surface of scorpion beta-toxins and elements that confer specificity for insect and mammalian voltage-gated sodium channels, J. Biol. Chem. 280 (2005) 5045–5053.